ChemComm

COMMUNICATION

View Article Online
View Journal | View Issue

Cite this: *Chem. Commun.*, 2016, 52, 13612

Received 7th August 2016,
Accepted 26th October 2016

DOI: 10.1039/c6cc08319f

www.rsc.org/chemcomm

Hydrogen evolution from glycerol aqueous solution under aerobic conditions over Pt/TiO_2 and Au/TiO_2 granular photocatalysts†

Hiroaki Sakurai,* Masato Kiuchi, Claire Heck and Tetsuro Jin

Hydrogen was efficiently evolved from glycerol aqueous solution upon vertical photoirradiation of a Pt/TiO_2 or Au/TiO_2 bed under aerobic conditions. Granular photocatalysts were easily deposited, leading to high H_2 selectivity (80–95%), whereas glycerol oxidation with CO_2 evolution became dominant when suspended powder photocatalysts were used.

Hydrogen is a clean-burning fuel that does not emit CO_2 even under combustion conditions. It can be considered an ideal energy storage medium because it can be produced by photocatalytic water-splitting using unlimited sunlight. An enormous amount of research has been conducted to identify a photocatalyst that is able to completely split pure water into hydrogen and oxygen.[1,2] However, a very high solar energy conversion efficiency has not yet been achieved, and the separation of simultaneously evolved H_2 and O_2 after the photocatalytic reaction is required. On the other hand, it has been reported that the addition of sacrificial electron donors, such as methanol[3] or carbohydrates,[4] greatly improves the efficiency of hydrogen evolution. Although CO_2 is released upon oxidation of the organic sacrificial agents, it can be considered as carbon neutral when biomass and its derivatives are used as sacrificial materials.[5] Thus, hydrogen production by using, for example, glycerol,[6] saccharides,[7] pyroligneous acid,[7] or castor oil[8] as sacrificial agents has been investigated so far.

These non-sacrificial water splitting and sacrificial hydrogen evolution reactions are mostly based on suspended photocatalyst powders under oxygen-free conditions, achieved by degassing or bubbling an inert gas through the system. It has been reported that reduction of dissolved oxygen may occur on the surface of the photocatalyst, which in some cases may decrease the photocatalytic activity for water splitting.[9,10] Generally, in aqueous solutions containing dissolved organic substances and high concentrations of oxygen, dissolved by air or oxygen bubbling, oxidative decomposition of the organic compounds to CO_2 becomes dominant and the evolution of hydrogen does not occur.[11] Thus, efficient H_2 production from water in open air is a challenging task.

In this study, we used typical photocatalysts, namely, Pt/TiO_2 and Au/TiO_2, to examine the hydrogen evolution from water exposed to air, with glycerol as a sacrificial agent. We found that continuous evolution of hydrogen can be achieved using a non-suspended granular catalyst, without bubbling of an inert gas. In addition, less CO_2 was produced under these conditions as compared with the CO_2 obtained under conventional suspended and oxygen-free reaction conditions.

Pt/TiO_2 and Au/TiO_2 were prepared by a photodeposition method, using TiO_2 powder (P25, Japan Aerosil) and a metal loading of 0.3 wt%, with chloroplatinic acid and chloroauric acid as precursors. After drying at 373 K, the photocatalysts formed hard aggregates with a heterogeneous particle size distribution. These aggregated particles were classified into aggregates A, B, and C (granular form, shown in Table 1) according to their size, as determined by sieving and sedimentation in water. A part of the aggregates was ground in a mortar to obtain aggregate D (powder form) with a size less than 10 μm in diameter. Hereafter, Pt/TiO_2 aggregate X will be referred to as Pt/TiO_2 (X), where X is A, B, C, or D. The size distribution of the catalyst particles was measured with a laser diffraction-scattering particle size distribution analyser.

The photocatalytic reaction was carried out using a borosilicate glass vial with a septum cap as the reaction vessel. As shown in Fig. S1 (ESI†), the vial was placed in a water bath

Table 1 Particle size distribution of Pt/TiO_2 photocatalysts

Photocatalyst aggregates	Nominal size range/μm	$d_{avr.}$/μm	$d_{10\%}$/μm	$d_{90\%}$/μm	Sedimentation rate/mm s^{-1}
Pt/TiO_2 (A)	300–710	450	308	614	182
Pt/TiO_2 (B)	125–300	174	75.5	281	27
Pt/TiO_2 (C)	40–125	82.3	48.4	121	6.1
Pt/TiO_2 (D)	—	5.7	3.0	9.5	0.029

National Institute of Advanced Industrial Science and Technology (AIST), 1-8-31 Ikeda, Osaka 563-8577, Japan. E-mail: h-sakurai@aist.go.jp

† Electronic supplementary information (ESI) available: Experimental details, Fig. S1–S8, Table S1, and a movie of hydrogen evolution. See DOI: 10.1039/c6cc08319f

(equipped with a Pyrex glass plate at the bottom) with temperature controlled at 293 K (reaction temperature T). The Xe lamp (500 W) output was filtered (wavelength range λ) and used as the light source. The radiation intensity (I) was measured by a thermopile. The vial was irradiated from the bottom (light-irradiated area S) by bending the output light beam using a mirror or a quartz optical fibre. A classified photocatalyst and an aqueous solution of glycerol (initial concentration C_0, volume V) were added, and the vial was sealed. The photocatalytic reaction was performed without bubbling an inert gas, in the presence of air in the headspace of the vial. The gas in the headspace was sampled with a gas-tight syringe, and H_2, O_2, and N_2 were analysed using a TCD gas chromatograph. CO_2 was determined using a FID gas chromatograph equipped with a methaniser. The amount of dissolved oxygen (DO) in the reaction solution was measured using a DO meter. Moreover, the turbidity of the reaction mixture due to the catalyst particles was measured using a turbidity sensor based on absorption spectrophotometry.

Fig. S2 (ESI†) shows the number-based size distribution of Pt/TiO_2 photocatalyst particles in water, measured by the laser diffraction method. Table 1 compares the size (mean diameter d_{avr}, 10% cumulative diameter $d_{10\%}$, and 90% cumulative diameter $d_{90\%}$) and the sedimentation rate of the aggregates. The primary particle size of P25 is about 20 nm.[12] The secondary particle size of Pt/TiO_2 (A), (B), and (C) was approximately consistent with the nominal size determined by the classification system used. Pt/TiO_2 (A) exhibited the largest diameter (d_{avr} = 450 μm), whereas Pt/TiO_2 (D) were found to be the smallest (d_{avr} = 5.7 μm). The sedimentation rate of the aggregates in water was calculated using the Stokes equation from the average particle size (Table 1), and was found to be very slow for the smallest particles. After stirring or shaking of the vial is stopped, Pt/TiO_2 (A), (B), and (C) sink to the bottom of the vial within 1 minute, whereas suspended Pt/TiO_2 (D) can be detected even after several tens of minutes. The aggregate size distribution of Au/TiO_2 (B) (Fig. S3, ESI†) was confirmed to be the same as that of Pt/TiO_2 (B).

TEM observations revealed that the particle size of the supported Pt was 3.7 ± 0.8 nm for Pt/TiO_2 (B) and 3.7 ± 0.9 nm for Pt/TiO_2 (D), indicating no variation for different Pt/TiO_2 aggregate sizes. The HAADF-STEM image (Fig. S4, ESI†) suggests that Pt particles are deposited not only on TiO_2 primary particles at the surface of the aggregates, but also on the TiO_2 particles inside the aggregates as well as in the gaps between the particles.

Although some large Au particles (>10 nm) were observed in the TEM image of Au/TiO_2 (C), powder X-ray diffraction showed only a broad peak of Au(311) at a 2θ angle of 77.6° (other Au peaks overlapped with the peaks of TiO_2). The crystallite size of Au calculated using the Scherrer equation, according to a previously reported method,[13] was 2.9 nm.

Upon Xe lamp irradiation of a glycerol solution containing Pt/TiO_2 (A), hydrogen-rich gas bubbles were generated continuously (Movie S1, ESI†). The time course of the reaction over Pt/TiO_2 (A), shown in Fig. 1, clearly demonstrates that H_2 is constantly evolved in the presence of O_2, both in the gas and liquid phases. The initial

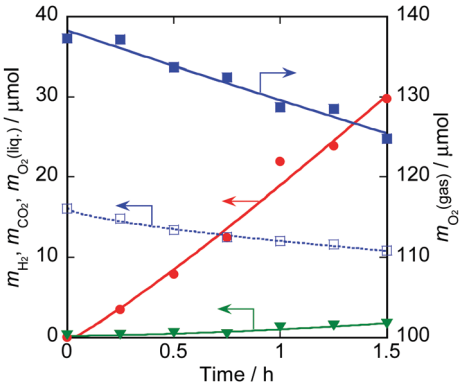

Fig. 1 Time course of H_2 (●), CO_2 (▼), and O_2 (■) amount in the gas phase and O_2 (□) amount in the liquid phase during the photocatalytic reaction. Pt/TiO_2 (A) 100 mg, C_0 = 1.09 mol L^{-1}, V = 85 mL, T = 293 K, S = 9.6 cm^2, λ > 320 nm, I = 285 mW cm^{-2}.

Table 2 Effect of the aggregate size of Pt/TiO_2 and mixing conditions of the solution on the photocatalytic activity[a]

Entry	Photocatalyst aggregates[b]	Mixing conditions[c]	Turbidity of the reaction mixture	Evolution rate/ μmol h^{-1}		
				H_2	CO_2	$-O_2$[d]
1	Pt/TiO_2 (A)	(1)	<10	16.6	2.5	0.3
2	Pt/TiO_2 (B)	(1)	<10	25.8	4.1	0.3
3	Pt/TiO_2 (C)	(1)	<10	34.2	6.5	1.0
4	Pt/TiO_2 (B)	(2)	~32	22.6	4.2	2.0
5	Pt/TiO_2 (B + D)[e]	(2)	548–1680	15.8	3.2	5.8
6	Pt/TiO_2 (D)	(3)	17 300	0.8	8.0	16.8

[a] Reaction conditions: C_0 = 5.43 × 10^{-2} mol L^{-1}, V = 5.0 mL, T = 293 K, S = 3.6 cm^2, λ = 320–690 nm, I = 137 mW cm^{-2}. [b] A–D are defined in Table 1, each 50 mg. [c] (1) no mixing, (2) shaking every 30 min, (3) stirring until homogeneous suspension. [d] O_2 consumption rate. [e] B (45 mg) + D (5 mg).

and final DO concentrations during the 1.5 h photocatalytic reaction were 6.05 and 4.05 mg L^{-1}, respectively, indicating that the reaction occurred under aerobic conditions. The H_2 selectivity in the evolved gas mixture (H_2 + CO_2) was calculated to be 95% from the formation rate of both gases.

Table 2 shows the effect of the mixing conditions on the rate of hydrogen evolution in air, using the Pt/TiO_2 photocatalyst. Upon using Pt/TiO_2 (A), (B), and (C), which were easily precipitated leaving a clear supernatant without mixing, the hydrogen evolution was predominant (entries 1–3). On the other hand, the H_2 evolution rate decreased with the increase in turbidity caused by the addition of Pt/TiO_2 (D) and mixing (entries 4–6). When using only Pt/TiO_2 (D) and under vigorous stirring to maintain a homogeneous suspension, little H_2 evolution was observed, and CO_2 generation by glycerol oxidation was dominant (entry 6). Suppression of H_2 evolution in the presence of dissolved oxygen when using a powdered Pt/TiO_2 photocatalyst and glucose or glycerol as sacrificial agents, and exclusive CO_2 gas evolution with O_2 flowing (20% O_2 in He) have been previously reported.[7,11]

A layer of Pt/TiO_2 (D) powder could not be obtained in the same manner as that of Pt/TiO_2 (A), (B), and (C), because turbidity was induced by a slight movement. In a different approach,

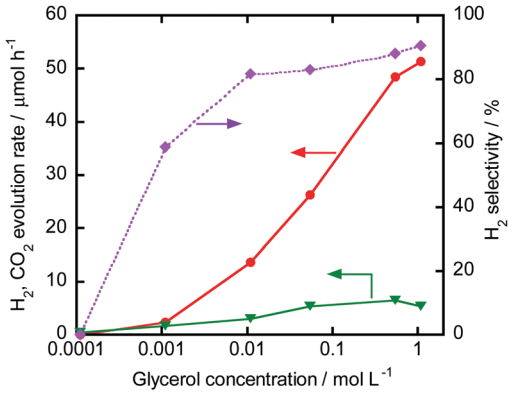

Fig. 2 Effect of glycerol concentration on the evolution rate of H_2 (●), CO_2 (▼), and the selectivity of H_2 (◆) in the evolved gas during photocatalytic reaction under aerobic conditions. Pt/TiO_2 (C) 50 mg, V = 5.0 mL, T = 293 K, S = 3.6 cm^2, $\lambda > 320$ nm, I = 285 mW cm^{-2}.

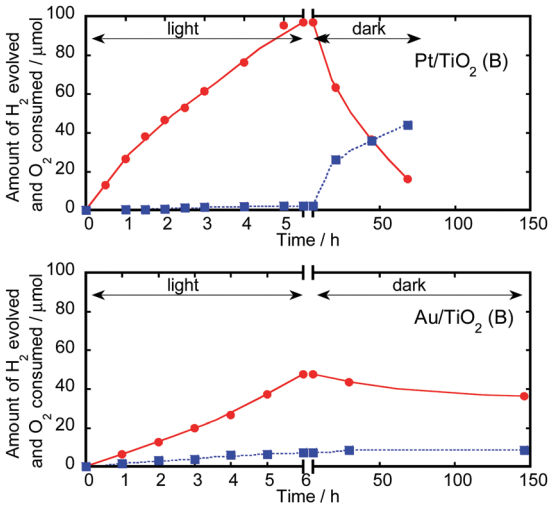

Fig. 3 Time course of H_2 evolution (●) and O_2 consumption (■) under light irradiation and under dark conditions. Pt/TiO_2 (B) or Au/TiO_2 (B) 50 mg, $C_0 = 5.43 \times 10^{-2}$ mol L^{-1}, V = 5.0 mL, T = 293 K, S = 3.6 cm^2, λ = 320–690 nm, I = 137 mW cm^{-2}.

the water was removed from the aqueous suspension of Pt/TiO_2 (D) by evaporation, to deposit a film of the powder at the bottom of the reaction vial. As a result, this film was found to be initially active for H_2 evolution with high (79%) selectivity (Fig. S5, ESI†). However, even without intentional mixing, the bed was not stable and the particles were partly suspended during the reaction, resulting in a decrease of H_2 selectivity (49% after 2 h reaction).

Fig. 2 shows the effect of the initial concentration of glycerol (C_0) on the reaction rate. The H_2 evolution rate increased linearly with log C_0. Such a dependence has been reported for glycerol, galactose, and ethanol sacrificial agents.[14] Moreover, for glycerol[15] and methanol,[16] this dependence is described by a reaction rate equation containing a Langmuir adsorption term. Our data in Fig. 2 can be well explained by Langmuir fitting (Fig. S6, ESI†), indicating that the surface was nearly saturated with adsorbed glycerol. The increase in CO_2 evolution rate with log C_0 was much smaller than that of H_2, resulting in an increase in H_2 selectivity with log C_0. The selectivity was over 80% for a C_0 of 0.01 mol L^{-1}, indicating that very low amounts of glycerol are effective.

H_2 evolution by photocatalytic activity of suspended particles in glycerol aqueous solution under an inert gas atmosphere has been widely investigated, and the observed H_2/CO_2 ratio was reported to be 7:3,[17,18] as expected from eqn (1).

$$C_3H_8O_3 + 3H_2O \rightarrow 7H_2 + 3CO_2 \quad (1)$$

A similar H_2 selectivity was observed in our control experiment (75% under N_2). In contrast, a significantly higher H_2 selectivity (80–95%) was obtained under our unique reaction conditions, despite the presence of oxygen. This suggests that partially oxidised glycerol compounds, such as aldehydes and carboxylic acids, may be formed during dehydrogenation.

Fig. 3 illustrates the time course of the reaction over Pt/TiO_2 (B) under light irradiation for about 6 hours and after stopping the irradiation. During the dark reaction, the H_2 and O_2 amounts in the headspace decreased, *i.e.* the evolved H_2 during initial 6 h decreased and the O_2 consumption increased. In another dark reaction over Pt/TiO_2 (A), both the dissolved and the gas phase O_2 amount decreased with the decrease of H_2 amount (Fig. S7, ESI†). Because the total amount of oxygen consumed was about 0.5–1.2 times the molar amount of hydrogen, in both experiments the backward reaction of dissolved oxygen and hydrogen (water regeneration) and the oxidation of glycerol or its partially oxidized derivatives should have occurred. As compared with the reaction over Pt/TiO_2, the H_2 evolution rate using similarly prepared Au/TiO_2 (B) was about half; however, a very small decrease in H_2 concentration was observed after stopping light irradiation (Fig. 3).

These differences can be explained by the difference in the activity of Pt and Au as thermal catalysts for H_2 oxidation. Metal oxide-supported Au nanoparticle thermal catalysts are well-known to exhibit a very high activity in CO oxidation reactions; however, they exhibit relatively low activity for H_2 oxidation, showing characteristics opposite to those of Pt and Pd catalysts (with high H_2 oxidation activity).[19] Iwase and co-workers examined the differences between Pt and Au cocatalysts in photocatalytic water splitting, and reported that the backward reaction over the Au cocatalyst under dark conditions was very slow.[20] The difference in the activity of these metal species in the backward reaction was also observed in our system. Fig. S8 (ESI†) shows the H_2 oxidation in pure water over Pt/TiO_2 (C), (D) and Au/TiO_2 (C), (D) after H_2 gas injection into the headspace of the vial, without light irradiation. The H_2 concentration was almost constant during the reaction over Au/TiO_2, whereas during the reaction over Pt/TiO_2 it decreased at different rates depending on the water mixing method and the aggregate size of the photocatalyst.

These differences highlight the importance of the thermal catalytic effect and the suppression of the backward reaction over Pt/TiO_2 even under light irradiation. Tabata *et al.* reported that, in the splitting of pure water under light irradiation from the top, the backward reaction is effectively suppressed.[21,22] They showed that, using a suspended Pt/TiO_2 catalyst powder, the evolved H_2 and O_2 immediately move to the gas phase and the

backward reaction is less likely to occur, considering that light penetrates the suspension layer only up to 0.2 mm. However, when H_2 and O_2 accumulate in the gas phase over time, they dissolve again into the liquid phase and diffuse to the region that is not reached by the light beam, thus regenerating water by thermal backward reaction. When the forward (water splitting) and backward (water regeneration) reactions come to equilibrium, H_2 and O_2 production apparently stops. In our work, the reaction is restricted within the sub-mm thick photocatalyst aggregate layer. It should be noted that, in this system, the backward reaction is more effectively suppressed, because of the absence of suspended photocatalyst particles in the liquid phase above the deposited photocatalyst layer.

On the other hand, we suggest that the aggregate structure of the photocatalyst also contributes to the suppression of the backward reaction. As mentioned above, the primary size of TiO_2 (P25) particles is about 20 nm, which aggregate to form secondary particles with sizes in the range of 40–700 μm. Upon generation of hydrogen by light irradiation, the interstitial space between the primary particles in the aggregate becomes anaerobic and therefore not susceptible to the oxygen in the liquid. A similar effect on the light-driven water splitting has been recently reported in a system consisting of hydrogenases and a Ru complex inside a porous glass plate.[23] In this system, hydrogen was efficiently generated even in ambient air because an anaerobic atmosphere was established inside the nanopores of the glass.

In another experiment, the rate of hydrogen evolution at 293 K under aerobic conditions was measured using a solar simulator (AM 1.5G). The solar-to-hydrogen conversion efficiency (STH) was calculated on the basis of the theoretical maximum energy that can be recovered from the produced hydrogen, using the following equation, described by Wang *et al.*:[24]

$$\mathrm{STH}\,(\%) = \frac{m_\mathrm{p} \cdot \Delta H_\mathrm{Liq.}}{I_\mathrm{s}} \times 100$$

where m_p is the rate of hydrogen evolution (mol s^{-1}), $\Delta H_\mathrm{Liq.}$ is the higher hydrogen heating value (286 kJ mol^{-1}), and I_s is the total incident solar irradiance. The STH values were calculated to be 1.04 and 0.42 for Pt/TiO_2 (C) and Au/TiO_2 (C), respectively, which are comparable to the STH recently reported for photocatalyst sheets with the Z-scheme system in pure water splitting.[25] It should be noted that a different definition for STH was used, and a comparison can be made only by applying the above definition (Table S1, ESI†).

In our method, the cost of the process can be significantly reduced because it does not require stirring of large amounts of water or costly inert gases for oxygen removal. The glycerol waste in the biodiesel production process can be beneficially used as a sacrificial agent. Various industrial wastewater components might also be effectively employed in the same way. Moreover, it is possible to further reduce the backward reaction by using a Au cocatalyst, minimising the decrease of hydrogen during dark conditions, *e.g.*, in cloudy weather or at night. All these advantageous characteristics make our system suitable for economical solar hydrogen production.

Acknowledgement is made to Dr K. Murai (AIST) for assistance with the solar simulator experiments, to Dr K. Asaka (AIST) for particle size measurements, and to Dr T. Uchida (AIST) for TEM observations.

Notes and references

1 A. Kudo and Y. Miseki, *Chem. Soc. Rev.*, 2009, **38**, 253–278.
2 R. Abe, *J. Photochem. Photobiol., C*, 2010, **11**, 179–209.
3 T. Kawai and T. Sakata, *Chem. Commun.*, 1980, 694–695.
4 T. Kawai and T. Sakata, *Nature*, 1980, **286**, 474–476.
5 K. Shimura and H. Yoshida, *Energy Environ. Sci.*, 2011, **4**, 2467–2481.
6 D. I. Kondarides, V. M. Daskalaki, A. Patsoura and X. E. Verykios, *Catal. Lett.*, 2008, **122**, 26–32.
7 S. Deguchi, N. Shibata, T. Takeichi, Y. Furukawa and N. Isu, *J. Jpn. Pet. Inst.*, 2010, **53**, 95–100.
8 S. Deguchi, T. Takeichi, S. Shimasaki, M. Ogawa and N. Isu, *AIChE J.*, 2011, **57**, 2237–2243.
9 K. Sayama and H. Arakawa, *J. Chem. Soc., Faraday Trans.*, 1997, **93**, 1647–1654.
10 K. Maeda, K. Teramura, H. Masuda, T. Takata, N. Saito, Y. Inoue and K. Domen, *J. Phys. Chem. B*, 2006, **110**, 13107–13112.
11 P. Panagiotopoulou, E. E. Karamerou and D. I. Kondarides, *Catal. Today*, 2013, **209**, 91–98.
12 O.-O. Prieto-Mahaney, N. Murakami, R. Abe and B. Ohtani, *Chem. Lett.*, 2009, **38**, 238–239.
13 H. Sakurai, K. Koga and M. Kiuchi, *Catal. Today*, 2015, **251**, 96–102.
14 D. I. Kondarides, V. M. Daskalaki, A. Patsoura and X. E. Verykios, *Catal. Lett.*, 2008, **122**, 26–32.
15 M. Li, Y. Li, S. Peng, G. Lu and S. Li, *Front. Chem. China*, 2009, **4**, 32–38.
16 A. Dickinson, D. James, N. Perkins, T. Cassidy and M. Bowker, *J. Mol. Catal. A: Chem.*, 1999, **146**, 211–221.
17 V. M. Daskalaki and D. I. Kondarides, *Catal. Today*, 2009, **144**, 75–80.
18 X. Fu, X. Wang, D. Y. C. Leung, Q. Gu, S. Chen and H. Huang, *Appl. Catal., B*, 2011, **106**, 681–688.
19 M. Haruta, S. Tsubota, T. Kobayashi, H. Kageyama, M. J. Genet and B. Delmon, *J. Catal.*, 1993, **144**, 175–192.
20 A. Iwase, H. Kato and A. Kudo, *Catal. Lett.*, 2006, **108**, 7–10.
21 S. Tabata, H. Nishida, Y. Masaki and K. Tabata, *Catal. Lett.*, 1995, **34**, 245–249.
22 S.-C. Moon, H. Mametsuka, S. Tabata and E. Suzuki, *Catal. Today*, 2000, **58**, 125–132.
23 T. Noji, M. Kondo, T. Jin, T. Yazawa, H. Osuka, Y. Higuchi, M. Nango, S. Itoh and T. Dewa, *J. Phys. Chem. Lett.*, 2014, **5**, 2402–2407.
24 Z. Wang, R. R. Roberts, G. F. Naterer and K. S. Gabriel, *Int. J. Hydrogen Energy*, 2012, **37**, 16287–16301.
25 Q. Wang, T. Hisatomi, Q. Jia, H. Tokudome, M. Zhong, C. Wang, Z. Pan, T. Takata, M. Nakabayashi, N. Shibata, Y. Li, I. D. Sharp, A. Kudo, T. Yamada and K. Domen, *Nat. Mater.*, 2016, **15**, 1–3.